www.lajss.org
Latin American Journal of Solids and Structures 3 (2006) 345–360

Straight fold analysis for axisymmetric crushing of thin walled frusta and tubes

M. Hosseini[1], H. Abbas[2,*] and N.K. Gupta[3]

[1]Dept. of Civil Engineering, Aligarh Muslim University, Aligarh, On leave from Dept. of Civil Engineering, Lorrestan University, Khorramabad, Iran
[2]Dept. of Civil Engineering, Aligarh Muslim University, Aligarh 202 002, India
[3]Dept. of Applied Mechanics, Indian Institute of Technology Delhi, New Delhi 110 016, India

Abstract

A straight fold model with partly inside and partly outside folding in axisymmetric crushing of thin metallic frusta has been presented. The first fold of the model ends at the mean diameter and all subsequent folds initiate and end at the mean diameter. Some parameters have been introduced for making the expressions valid for all the folds. Existing total outside fold model of frusta and partly inside and partly outside fold model of tube can be derived from the present model. The relations for obtaining the inside and outside fold lengths in tubes are derived. Different values of yield stress of the material in compression and tension have been taken in the analysis. The variation of circumferential strain during the formation of a fold has been taken into account for the purpose of computing the variation of crushing load. The results have been compared with experiments and good agreement has been observed.

Keywords: frusta, tubes, crushing, folding, straight-fold

1 Introduction

The collapse behaviour of tubes and frusta has been studied in the past [1–10, 12–15] for their application in the design of crash energy absorbing devices. The pioneering work in this direction was done by Alexander [6] who gave an analysis for axisymmetric crushing of cylindrical tubes by the formation of straight folds with energy absorption in bending localized at the hinges formed at the junctions of the limbs of folds. He obtained expressions for the fold length and the mean crushing load by minimizing the total energy absorbed in bending and circumferential deformation. This analysis formed the basis of many later studies [1–5, 7–10, 12–15].

The mechanics of crushing phenomenon is quite complex and not amenable to complete analytical solution. It has been observed in experiments that when tubes deform in axisymmetric mode, the fold formed is partly inside and partly outside the initial tube diameter [9, 10, 14],

*Corresp. author email: abbas_husain@hotmail.com Received 30 March 2006; In revised form 17 June 2006

whereas, frusta deforms in axisymmetric mode by outside folding [8]. Analytical solutions available are not many and those available have made several simplifying assumptions which include the deformation to be inextensional and the fold to be only outside [4] or inside [2,3] the initial diameter of the tube. These analyses only determined the mean collapse load for which mean circumferential strain was enough. It is because the circumferential strain varies with the rotation of Analysis available [13,14], which considered inside/outside folding in tubes assumed that both parts are equal in length. Experiments have shown that this is not true and the inner fold is smaller than the outer fold in tubes [1,7,9,10,13]. The upper limb of first fold connects with initial line of the tube only for the total outside and total inside fold models. Whereas for the models in which the folding is partly inside and partly outside, the upper limb of the first fold does not connect with the initial line of the tube. In the present paper, a third partial limb is introduced to address this problem.

In the present paper, an analytical straight fold model with three limbs is presented for axisymmetric crushing of frusta with partly inside and partly outside folding based on energy considerations. The model developed considers the variation of circumferential strain during the formation of a fold and the difference in yield strength of material in tension and compression. The existing total outside fold model of frusta [8] and the partly inside and partly outside fold models [10] have been derived from the proposed model. The mean and the variation of crushing load for frusta and tubes have been computed. The results have been compared with experiments and reasonably good agreement has been observed. The results are of help in understanding the phenomenon of actual fold formation.

2 Analysis of frusta

We consider a thin frustum of thickness t, smaller end radius R_1, and angle of taper α, as shown in Fig. 1. The axisymmetric crushing of the frustum is also shown in this figure, by the formation of partly inside and partly outside straight folding. The folding model adopted in the present analysis is shown in Fig. 1. It can be seen from Fig. 1 that there are three limbs in the model instead of two taken in the earlier model [11]. After the completion of the second fold, the first limb of second fold gets in line with the third limb of the first fold thus the hinge at their junction located at the initial line of the frusta gets eliminated.

The bottom portion of frustum a'-b'-c'-d'-e'-f' in undeformed state assumes the shape a-b-c-d-e-f after axisymmetric crushing. In the first fold, the length of first and second limbs are h_1 and h_2 respectively out of which mh_1, mh_2 are inside the initial line of frustum for first and second limbs respectively, where m is the folding parameter. The length of third limb is mh_1, which is inside the initial line of the tube. In the second and other subsequent folds, the length of first limb is (1-m)h_1, second is h_2 and the third is mh_1. The relationship between the lengths of the limbs can be obtained from the geometry in complete crushed state:

$$h_1 = Kh_2 \tag{1}$$

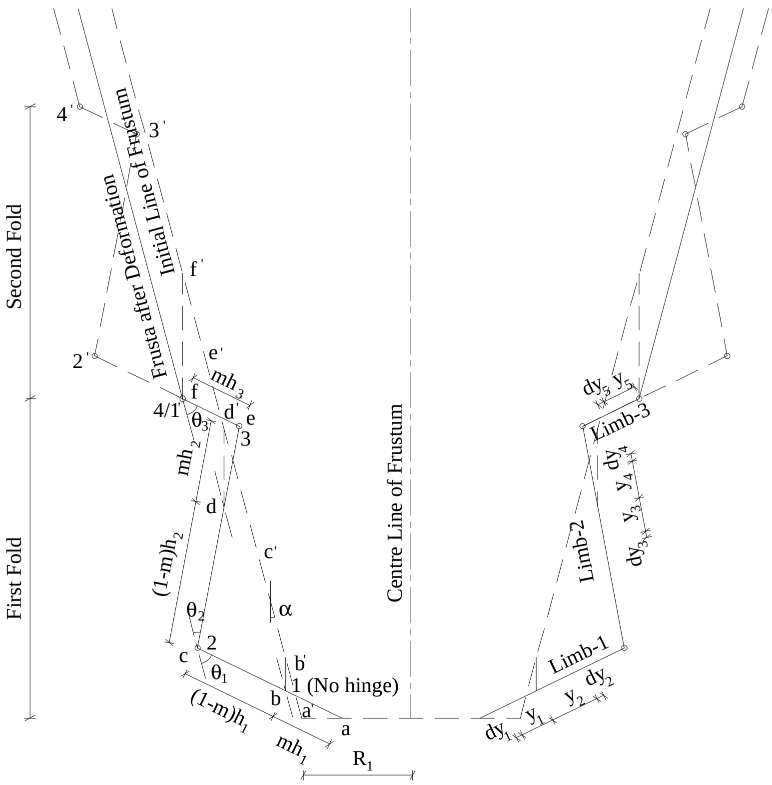

Figure 1: Axial crushing model of frusta

where,

$$K = \frac{1+\sin\alpha}{1-\sin\alpha} \tag{2}$$

The total vertical crushed length of first fold is (1+m)$h_1 + h_2$ and its value for other folds is $h_1 + h_2$ as shown in Fig. 1. The angle of inclination of the limbs of the fold, θ_1, θ_2 and θ_3 have been measured from the initial line of the frustum, thus their initial value in the undeformed state is zero and their maximum value after complete crushing is (π/2-α), (π/2+α) and (π/2-α) respectively. It is seen from geometry that the angle θ_3 is equal to angle θ_1. In the present analysis, complete crushing of the fold has been assumed because the consideration of effective crushing distance [3] is coupled with the reduction in the energy dissipation. The yield strength of the material of the frustum in compression and tension has been taken as f_{yc} and f_{yt} respectively, and $r = f_{yc}/f_{yt}$.

The plastic moment of resistance of the material of the frustum has been taken as $M_p = \frac{1}{2\sqrt{3}} f_{yt} t_0^2$.

2.1 Energy absorption in crushing

The radii of the points a, b, c, d, e and f in the deformed state of the frustum (Fig. 1) are given by:

$$R_a = R_1 + mh_1 \left\{ \sin\alpha - \sin\left(\theta_1 + \alpha\right) \right\} \tag{3}$$

$$R_b = R_1 + mh_1 \sin\alpha \tag{4}$$

$$R_c = R_1 + h_1 \left\{ m \sin\alpha + (1-m)\sin\left(\theta_1 + \alpha\right) \right\} \tag{5}$$

$$R_d = R_1 + \left\{ h_1 + (1-m)\, h_2 \right\} \sin\alpha \tag{6}$$

$$R_e = R_1 + \left\{ h_1 + (1-m)\, h_2 \right\} \sin\alpha - mh_2 \sin\left(\theta_2 - \alpha\right) \tag{7}$$

$$R_f = R_1 + \left\{ h_1 + h_2 + mh_3 \right\} \sin\alpha \tag{8}$$

Also,

$$R_d = R_1 + h_1 \left\{ m \sin\alpha + (1-m)\sin\left(\theta_1 + \alpha\right) \right\} - (1-m)\, h_2 \sin\left(\theta_2 - \alpha\right) \tag{9}$$

which gives relation between the two angles:

$$\theta_2 = \sin^{-1}\left[K \sin(\theta_1 + \alpha) - (K+1)\sin\alpha \right] - \alpha \tag{10}$$

For the second fold, the above radii will be such that the new value of R_1 is $R_1 + (h_1 + h_2 + mh_3)\sin\alpha$.

The energy dissipation in flexure has been assumed to be localized at the hinges which is in the form of rotation at lower, upper and intermediate plastic hinges. The energy dissipated in plastic bending $W_{b\theta}$, in the rotation of the first and third limb upto angle θ_1 and the second limb upto angle θ_2 is given by:

$$\begin{aligned} W_{b\theta} &= 2\pi M_p \left[\underbrace{a_2 \int_0^{\theta_1} R_f d\theta_1}_{\text{(Hinge-4)}} + \underbrace{a_2 \int_0^{\theta_1} R_e d\theta_1 + \int_0^{\theta_2} R_e d\theta_2}_{\text{(Hinge-3)}} + \underbrace{\int_0^{\theta_2} R_c d\theta_2 + \int_0^{\theta_2} R_c d\theta_1}_{\text{(Hinge-2)}} + \underbrace{a_1 \int_0^{\theta_1} R_b d\theta_1}_{\text{(Hinge-1)}} \right] \\ &= 2\pi M_p \left[\int_0^{\theta_3} a_2 \left(R_f + R_e\right) d\theta_3 + \int_0^{\theta_2} \left(R_c + R_e\right) d\theta_2 + \int_0^{\theta_1} \left(a_1 R_b + R_c\right) d\theta_1 \right] \end{aligned} \tag{11}$$

During the formation of first fold, lower hinge does not exist, whereas it exists in subsequent folds. It has been incorporated in the above expression by introducing a constant, a_1. Its value will be zero (i.e. $a_1 = 0$) for first and unity (i.e. $a_1 = 1$) for rest of the folds. For total outside fold model, third limb does not exist, which has been incorporated by introducing a parameter

a_2 in the above expression. The parameter a_2 will be zero for the total outside fold model (i.e. m=0) else it will be unity. Evaluating the integrals, $W_{b\theta}$ is obtained as

$$W_{b\theta} = 2\pi M_p \begin{bmatrix} \{(a_1 + 2a_2 + 1)\,\theta_1 + 2\theta_2\}\, R_1 + mKh_2\,(a_1 + 2a_2 + 1)\,\theta_1 \sin\alpha \\ +Kh_2\,(1 - m - ma_2)\,\{\cos(\theta_1 + \alpha) - \cos\alpha\} + (1 - 2m)\,h_2 \cos\alpha \\ +2h_2\,\{(1 + K)\,(a_2\theta_1 + \theta_2) - m\theta_2\}\sin\alpha - (1 - 2m)\,h_2 \cos(\theta_2 - \alpha) \end{bmatrix} \tag{12}$$

putting, $\theta_1 = \frac{\pi}{2} - \alpha$ and $\theta_2 = \frac{\pi}{2} + \alpha$ in the above equation gives the total energy absorbed in flexure during complete crushing of the fold:

$$W_b = 2\pi M_p h_2 X \tag{13}$$

where,

$$X = \begin{bmatrix} (a_1 + 2a_2 + 1)\left(\frac{\pi}{2} - \alpha\right)\left(\frac{R_1}{h_2} + mK\sin\alpha\right) + \cos\alpha \\ + \{(1 + K)\,\{a_2\,(\pi - 2\alpha) + (\pi + 2\alpha)\}\}\sin\alpha - 2m\cos\alpha \\ + (\pi + 2\alpha)\left(\frac{R_1}{h_2} - m\sin\alpha\right) + K\,(1 - m - ma_2)\cos\alpha \end{bmatrix} \tag{14}$$

which for m= 0 and $a_2 = 0$ converts to the total outside fold model of frusta [14]:

$$W_b = 2\pi M_p \left[\left\{(a_1 + 3)\,\frac{\pi}{2} - \alpha\,(a_1 - 1)\right\} R_1 + h_2\,(1 + K)\,\{(\pi + 2\alpha)\sin\alpha + \cos\alpha\}\right] \tag{15}$$

and for αg 0, $a_2 = 1$ and $h_1 = h_2 = h$ (say), converts to the partly inside and partly outside model of cylinder of radius R_1 [12]:

$$W_b = 2\pi M_p \left[(a_1 + 5)\,\frac{\pi}{2} R_1 + 2h\,(1 - 2m)\right] \tag{16}$$

The energy dissipated in circumferential stretching for the portion of the fold going inside the initial diameter of the frustum and circumferential compression for the portion of the fold going outside and rotation upto an angle θ_1 for first and third limbs and θ_2 for the second limb of the fold, $W_{c\theta}$, can be calculated by:

$$W_{c\theta} = \underbrace{\int_0^{\theta_1} \left(\frac{dW_{c1}}{d\theta_1}\right) d\theta_1}_{\text{(First Limb)}} + \underbrace{\int_0^{\theta_2} \left(\frac{dW_{c2}}{d\theta_2}\right) d\theta_2}_{\text{(Second Limb)}} + \underbrace{\int_0^{\theta_1} \left(\frac{dW_{c3}}{d\theta_1}\right) d\theta_1}_{\text{(Third Limb)}} \tag{17}$$

Considering an element of width dy_1 at a distance y_1 from point b in the portion of the first limb going inside and another element of width dy_2 at a distance y_2 from point b in the portion of the first limb going outside. It is to be noted here that the portion of limb going inside the initial line of frusta does not exist in the second and subsequent folds, which has been incorporated for introducing a parameter a_3 in the expressions of energy dissipation. Its value will be unity for the first fold and zero for other folds. The energy dissipated in circumferential deformation can be calculated as follows:

$$\frac{dW_{c1}}{d\theta_1} = a_3 \int_0^{mh_1} f_y t_0 \left(\left| \frac{d\varepsilon_1}{d\theta_1} \right| \right) dA_1 + \int_0^{(1-m)h_1} f_y t_0 \left(\left| \frac{d\varepsilon_2}{d\theta_1} \right| \right) dA_2 \tag{18}$$

where, dA_1 and dA_2 are the area of elemental rings, given by

$$dA_1 = 2\pi \left\{ R_b - y_1 \sin(\theta_1 + \alpha) \right\} dy_1 \text{ and } dA_2 = 2\pi \left\{ R_b + y_2 \sin(\theta_1 + \alpha)) \right\} dy_2 \tag{19}$$

and ε_1 and ε_2 are the circumferential strains in the two elements, given by

$$\varepsilon_1 = \frac{2\pi \left[\left\{ R_b - y_1 \sin(\theta_1 + \alpha) \right\} \right] - (R_b - y_1 \sin\alpha)}{2\pi (R_b - y_1 \sin\alpha)} \tag{20}$$

$$\varepsilon_2 = \frac{2\pi \left[\left\{ R_b + y_2 \sin(\theta_1 + \alpha) \right\} \right] - (R_b + y_2 \sin\alpha)}{2\pi (R_b + y_2 \sin\alpha)} \tag{21}$$

Differentiating the above two equations, we get,

$$\frac{d\varepsilon_1}{d\theta_1} = -\frac{y_1 \cos(\theta_1 + \alpha)}{R_b - y_1 \sin\alpha} \tag{22}$$

$$\frac{d\varepsilon_2}{d\theta_1} = \frac{y_2 \cos(\theta_1 + \alpha)}{R_b + y_2 \sin\alpha} \tag{23}$$

Using Eq. (19), (22) and (23), Eq. (18) gives,

$$\frac{dW_{c1}}{d\theta_1} = 2\pi f_y t_0 \left(\frac{R_b}{\sin\alpha} \right)^2 \left[\begin{array}{l} \left\{ -\ln(A^{ra_3} B) + (1 - m - rma_3) \frac{h_1 \sin\alpha}{R_b} \right\} \cos(\theta_1 + \alpha) \\ + \left\{ \begin{array}{l} 2\ln(A^{ra_3} B) + ra_3 A^2 + B^2 - (1 + ra_3) \\ -4(1 - m - rma_3) \frac{h_1 \sin\alpha}{R_b} \end{array} \right\} \frac{\sin 2(\theta_1 + \alpha)}{4\sin\alpha} \end{array} \right] \tag{24}$$

where,

$$A = 1 - \frac{mh_1 \sin\alpha}{R_b} \text{ and } B = 1 + \frac{(1 - m) h_1 \sin\alpha}{R_b} \tag{25}$$

Considering an element of width dy_3 at a distance y_3 from point d in the portion of the second limb going inside and another element of width dy_4 at a distance y_4 from point d in the portion of the second limb going outside, the energy dissipated in circumferential deformation can be calculated as follows:

$$\frac{dW_{c2}}{d\theta_2} = \int_0^{(1-m)h_2} f_y t_0 \left(\left| \frac{d\varepsilon_3}{d\theta_2} \right| \right) dA_3 + \int_0^{mh_2} f_y t_0 \left(\left| \frac{d\varepsilon_4}{d\theta_2} \right| \right) dA_4 \tag{26}$$

where,

$$dA_3 = 2\pi \left\{ R_d + y_3 \sin(\theta_2 - \alpha) \right\} dy_3 \text{ and } dA_4 = 2\pi \left\{ R_d - y_4 \sin(\theta_2 - \alpha) \right\} dy_4 \tag{27}$$

$$\varepsilon_3 = \frac{2\pi \left[\left\{ R_d + y_3 \sin(\theta_2 - \alpha) \right\} \right] - (R_d - y_3 \sin\alpha)}{2\pi (R_d - y_3 \sin\alpha)} \tag{28}$$

$$\varepsilon_4 = \frac{2\pi \left[\left\{ R_d - y_4 \sin(\theta_2 - \alpha) \right\} \right] - (R_d + y_4 \sin\alpha)}{2\pi (R_d + y_4 \sin\alpha)} \tag{29}$$

Differentiating the above two equations, we get,

$$\frac{d\varepsilon_3}{d\theta_2} = \frac{y_3 \cos(\theta_2 - \alpha)}{R_d - y_3 \sin\alpha} \tag{30}$$

$$\frac{d\varepsilon_4}{d\theta_2} = -\frac{y_4 \cos(\theta_2 - \alpha)}{R_d + y_4 \sin\alpha} \tag{31}$$

Using Eq. (27), (30) and (31), Eq. (26) gives,

$$\frac{dW_{c2}}{d\theta_2} = -2\pi f_y t_0 \left(\frac{R_d}{\sin\alpha} \right)^2 \left[\begin{array}{l} \left\{ \ln(C^r D) + (1 - m - rm) \frac{h_2 \sin\alpha}{R_d} \right\} \cos(\theta_2 - \alpha) \\ + \left\{ \begin{array}{l} 2\ln(C^r D) + rC^2 + D^2 - (1 + r) \\ +4(1 - m - rm) \frac{h_2 \sin\alpha}{R_d} \end{array} \right\} \frac{\sin 2(\theta_2 - \alpha)}{4 \sin\alpha} \end{array} \right] \tag{32}$$

where,

$$C = 1 - \frac{(1 - m) h_2 \sin\alpha}{R_d} \text{ and } D = 1 + \frac{m h_2 \sin\alpha}{R_d} \tag{33}$$

Considering an element of width dy_5 at a distance y_5 from point f in the third limb, the energy dissipated in circumferential compression can be calculated as follows:

$$\frac{dW_{c3}}{d\theta_1} = \int_0^{mh_3} f_y t_0 \left(\left| \frac{d\varepsilon_5}{d\theta_1} \right| \right) dA_5 \tag{34}$$

where,

$$dA_5 = 2\pi \left\{ R_f - y_5 \sin(\theta_1 + \alpha) \right\} dy_5 \tag{35}$$

$$\varepsilon_5 = \frac{2\pi \left[\left\{ R_f - y_5 \sin(\theta_1 + \alpha) \right\} \right] - (R_f - y_5 \sin\alpha)}{2\pi (R_f - y_5 \sin\alpha)} \tag{36}$$

Differentiating the above equation, gives

$$\frac{d\varepsilon_5}{d\theta_1} = -\frac{y_5 \cos(\theta_1 + \alpha)}{R_f - y_5 \sin\alpha} \tag{37}$$

Using Eq. (35) and (37), Eq. (34) gives,

$$\frac{dW_{c3}}{d\theta_1} = 2\pi f_y t_0 \left(\frac{R_f}{\sin\alpha}\right)^2 \left[\begin{array}{l} \left\{\ln\left(E^r\right) + rm\frac{h_1\sin\alpha}{R_f}\right\}\cos\left(\theta_1+\alpha\right) \\ +\left\{\begin{array}{l} 2\ln\left(E^r\right) + rE^2 - r \\ +4rm\frac{h_1\sin\alpha}{R_f} \end{array}\right\}\frac{\sin 2(\theta_1+\alpha)}{4\sin\alpha} \end{array}\right] \tag{38}$$

where,

$$E = 1 - \frac{mh_1\sin\alpha}{R_f} \tag{39}$$

Using Eqs. (24), (32) and (38), Eq. (17) gives the energy absorbed in circumferential deformation during the rotation of first and third limb upto θ_1 and second limb upto θ_2:

$$\begin{aligned} W_{C\theta} = {} & 2\pi f_y t_0 \left(\frac{R_b}{\sin\alpha}\right)^2 \left[\begin{array}{l} \left\{-\ln\left(A^{ra_3}B\right) + \left(1-m-rma_3\right)\frac{h_1\sin\alpha}{R_b}\right\}\left\{\sin\left(\theta_1+\alpha\right)-\sin\alpha\right\} \\ +\left\{\begin{array}{l} 2\ln\left(A^{ra_3}B\right) + ra_3A^2 + B^2 - \left(1+ra_3\right) \\ -4\left(1-m-rma_3\right)\frac{h_1\sin\alpha}{R_b} \end{array}\right\}\left\{\frac{\cos 2\alpha - \cos 2(\theta_1+\alpha)}{8\sin\alpha}\right\} \end{array}\right] \\ & - 2\pi f_y t_0 \left(\frac{R_d}{\sin\alpha}\right)^2 \left[\begin{array}{l} \left\{\ln\left(C^rD\right) + \left(1-m-rm\right)\frac{h_2\sin\alpha}{R_d}\right\}\left\{\sin\left(\theta_2-\alpha\right)-\sin\alpha\right\} \\ +\left\{\begin{array}{l} 2\ln\left(C^rD\right) + rC^2 + D^2 - \left(1+r\right) \\ +4\left(1-m-rm\right)\frac{h_2\sin\alpha}{R_d} \end{array}\right\}\left\{\frac{\cos 2\alpha - \cos 2(\theta_2-\alpha)}{8\sin\alpha}\right\} \end{array}\right] \\ & + 2\pi f_y t_0 \left(\frac{R_f}{\sin\alpha}\right)^2 \left[\begin{array}{l} \left\{\ln\left(E^r\right) + rm\frac{h_1\sin\alpha}{R_f}\right\}\left\{\sin\left(\theta_1+\alpha\right)-\sin\alpha\right\} \\ +\left\{\begin{array}{l} 2\ln\left(E^r\right) + rE^2 - r \\ +4rm\frac{h_1\sin\alpha}{R_f} \end{array}\right\}\left\{\frac{\cos 2\alpha - \cos 2(\theta_1+\alpha)}{8\sin\alpha}\right\} \end{array}\right] \end{aligned} \tag{40}$$

putting, $\theta_1 = \frac{\pi}{2} - \alpha$ and $\theta_2 = \frac{\pi}{2} + \alpha$ in the above equation gives the total energy absorbed in circumferential deformation during complete crushing of the fold:

$$W_c = 2\pi f_y t_0 \frac{1-\sin\alpha}{\sin^2\alpha}\left[Y+Z\right] \tag{41}$$

where,

$$Y = R_b^2A_1 - R_d^2A_2 + R_f^2A_3 \tag{42}$$

$$Z = \frac{1+\sin\alpha}{4\sin\alpha}\left\{R_b^2B_1 - R_d^2B_2 + R_f^2B_3\right\} \tag{43}$$

$$A_1 = -\ln\left(A^{ra_3}B\right) + \left(1-m-mra_3\right)Kh_2\frac{\sin\alpha}{R_b} \tag{44}$$

$$A_2 = \ln\left(C^rD\right) + \left(1-m-mr\right)h_2\frac{\sin\alpha}{R_d} \tag{45}$$

$$A_3 = \ln\left(E^r\right) + rmKh_2\frac{\sin\alpha}{R_f} \tag{46}$$

$$B_1 = -\left(1 + ra_3\right) + B^2 + ra_3 A^2 + 2\ln\left(A^{ra_3} B\right) - 4\left(1 - m - mra_3\right) K h_2 \frac{\sin\alpha}{R_b} \tag{47}$$

$$B_2 = -\left(1 + r\right) + D^2 + rC^2 + 2\ln\left(C^r D\right) + 4\left(1 - m - mr\right) h_2 \frac{\sin\alpha}{R_d} \tag{48}$$

$$B_3 = -r + rE^2 + 2\ln\left(E^r\right) + 4rmKh_2 \frac{\sin\alpha}{R_f} \tag{49}$$

which for total outside fold model (i.e. m=0) converts to the expression given in Ref. [8]. Eq. (40) is not valid for αg 0, for which, we get,

$$W_c = \pi f_{yt} t_0 h^2 \left[\left(a_3 + 2\right) rm^2 \left(1 - \frac{mh}{3R_1}\right) + 2\left(1 - m\right)^2 \left\{1 + \frac{\left(1 - m\right) h}{3R_1}\right\}\right] \tag{50}$$

which is same as that given in Ref. [12] for cylinder of radius R_1 and size of fold, h.

2.2 Average crushing load

Assuming that the energy dissipation in the axisymmetric axial crushing of frusta takes place in the form of flexural and circumferential deformations, therefore, the external work done can be equated to the energy absorbed in bending and circumferential stretching. The average crushing load, P_m, can, therefore, be calculated:

$$P_m = \frac{W_b + W_c}{\left\{1 + K\left(1 + a_4 m\right)\right\} h_2 \cos\alpha} \tag{51}$$

where, parameter a_4 will be unity for first fold and zero for other folds; W_b is given by Eq. (13) and W_c is given by Eq. (41) for frusta and Eq. (50) for tubes. For frusta, Eq. (51) converts to:

$$P_m = \frac{\pi f_y t_0^2 X}{\sqrt{3}\left\{1 + K\left(1 + a_4 m\right)\right\}\cos\alpha} + \frac{2\pi f_y t_0}{h_2\left\{1 + K\left(1 + a_4 m\right)\right\}} \frac{1 - \sin\alpha}{\sin^2\alpha\cos\alpha}\left[Y + Z\right] \tag{52}$$

and for tube, Eq. (51) gives:

$$\begin{aligned} P_m = & \frac{\pi f_y t_0^2 \left[R_1\left(a_1 + 2a_2 + 3\right)\frac{\pi}{2} + h\left(2 - 3m - ma_2\right)\right]}{\sqrt{3} h\left\{1 + K\left(1 + a_4 m\right)\right\}\cos\alpha} \\ & + \frac{\pi f_y t_0 h\left[\left(a_3 + 2\right) rm^2\left(1 - \frac{mh}{3R_1}\right) + 2\left(1 - m\right)^2\left\{1 + \frac{(1-m)h}{3R_1}\right\}\right]}{\left\{1 + K\left(1 + a_4 m\right)\right\}\cos\alpha} \end{aligned} \tag{53}$$

2.3 Size of fold and folding parameter, m

Determination of the size of fold, h_1 and h_2, and the folding parameter, m, requires the minimization of external work done for crushing unit length of frusta during the fold formation or the minimization of average crushing load of the fold i.e.

$$\frac{\partial P_m}{\partial h_2} = 0 \tag{54}$$

and

$$\frac{\partial P_m}{\partial m} = 0 \tag{55}$$

where, P_m is given by Eq. (52) for frusta. Putting the value of P_m from Eq. (52), Eq. (54) converts to:

$$\frac{t_0}{\sqrt{3}}\frac{\partial X}{\partial h_2} + \frac{2\,(1-\sin\alpha)}{\sin^2\alpha}\frac{\partial}{\partial h_2}\left[\frac{Y+Z}{h_2}\right] = 0 \tag{56}$$

where,

$$\frac{\partial X}{\partial h_2} = -\left[(a_1+2a_2+1)\left(\frac{\pi}{2}-\alpha\right)+(\pi+2\alpha)\right]\frac{R_1}{h_2^2} \tag{57}$$

$$\frac{\partial}{\partial h_2}\left[\frac{Y}{h_2}\right] = \frac{1}{h_2}\left[-\frac{Y}{h_2} + R_b^2\frac{dA_1}{dh_2} - R_d^2\frac{dA_2}{dh_2} + R_f^2\frac{dA_3}{dh_2}\right] \tag{58}$$

$$\frac{\partial}{\partial h_2}\left[\frac{Z}{h_2}\right] = \frac{1}{h_2}\left[-\frac{Z}{h_2} + \frac{1+\sin\alpha}{4\sin\alpha}\left(R_b^2\frac{dB_1}{dh_2} - R_d^2\frac{dB_2}{dh_2} + R_f^2\frac{dB_3}{dh_2}\right)\right] \tag{59}$$

$$\frac{dA_1}{dh_2} = -\left[ra_3B\frac{dA}{dh_2} + A\frac{dB}{dh_2}\right]\frac{1}{AB} + (1-m-mra_3)\,K\frac{\sin\alpha}{R_b} \tag{60}$$

$$\frac{dA_2}{dh_2} = \left[rD\frac{dC}{dh_2} + C\frac{dD}{dh_2}\right]\frac{1}{CD} + (1-m-mr)\,\frac{\sin\alpha}{R_d} \tag{61}$$

$$\frac{dA_3}{dh_2} = \left[r\frac{dE}{dh_2}\right]\frac{1}{E} + rmK\frac{\sin\alpha}{R_f} \tag{62}$$

$$\frac{dB_1}{dh_2} = 2\left[ra_3\left(A+\frac{1}{A}\right)\frac{dA}{dh_2} + \left(B+\frac{1}{B}\right)\frac{dB}{dh_2} - 2\,(1-m-mra_3)\,K\frac{\sin\alpha}{R_b}\right] \tag{63}$$

$$\frac{dB_2}{dh_2} = 2\left[r\left(C+\frac{1}{C}\right)\frac{dC}{dh_2} + \left(D+\frac{1}{D}\right)\frac{dD}{dh_2} + 2\,(1-m-mr)\,\frac{\sin\alpha}{R_d}\right] \tag{64}$$

$$\frac{dB_3}{dh_2} = 2r\left[E+\frac{1}{E} + 2mK\frac{\sin\alpha}{R_f}\right] \tag{65}$$

$$\frac{dA}{dh_2} = -mK\frac{\sin\alpha}{R_b}, \quad \frac{dB}{dh_2} = (1-m)\,K\frac{\sin\alpha}{R_b}, \quad \frac{dC}{dh_2} = -\,(1-m)\,\frac{\sin\alpha}{R_d} \tag{66}$$

$$\frac{dD}{dh_2} = m\frac{\sin\alpha}{R_d}, \quad \frac{dE}{dh_2} = -mK\frac{\sin\alpha}{R_f} \tag{67}$$

Putting the value of P_m from Eq. (52) for frusta, Eq. (57) converts to:

$$\frac{t_0}{\sqrt{3}}\frac{d}{dm}\left[\frac{X}{1+K\,(1+a_4m)}\right] + \frac{2\,(1-\sin\alpha)}{h_2\sin^2\alpha}\frac{d}{dm}\left[\frac{Y+Z}{1+K\,(1+a_4m)}\right] = 0 \tag{68}$$

$$\frac{d}{dm}\left[\frac{X}{1+K\,(1+a_4m)}\right] = \frac{1}{[1+K\,(1+a_4m)]^2}\left[\{1+K\,(1+a_4m)\}\frac{dX}{dm} - a_4KX\right] \tag{69}$$

$$\frac{d}{dm}\left[\frac{Y+Z}{1+K\left(1+a_{4}m\right)}\right]=\frac{1}{\left[1+K\left(1+a_{4}m\right)\right]^{2}}\left[\left\{1+K\left(1+a_{4}m\right)\right\}\frac{d\left(Y+Z\right)}{dm}-a_{4}KYZ\right] \tag{70}$$

$$\frac{\partial X}{\partial m}=h_{2}\left[\begin{array}{l} K\left(a_{1}+2a_{2}+1\right)\left(\frac{\pi}{2}-\alpha\right)\sin\alpha-2\cos\alpha \\ -\left(\pi+2\alpha\right)\sin\alpha-K\left(1+a_{2}\right)\cos\alpha \end{array}\right] \tag{71}$$

$$\frac{\partial Y}{\partial m}=R_{b}^{2}\frac{dA_{1}}{dm}-R_{d}^{2}\frac{dA_{2}}{dm}+R_{f}^{2}\frac{dA_{3}}{dm} \tag{72}$$

$$\frac{\partial Z}{\partial m}=\frac{1+\sin\alpha}{4\sin\alpha}\left[R_{b}^{2}\frac{dB_{1}}{dm}-R_{d}^{2}\frac{dB_{2}}{dm}+R_{f}^{2}\frac{dB_{3}}{dm}\right] \tag{73}$$

$$\frac{dA_{1}}{dm}=-\left[\frac{ra_{3}}{A}+\frac{1}{B}-\left(1+ra_{3}\right)\right]\frac{dA}{dm} \tag{74}$$

$$\frac{dA_{2}}{dm}=\left[\frac{r}{C}+\frac{1}{D}-\left(1+r\right)\right]\frac{dC}{dm} \tag{75}$$

$$\frac{dA_{3}}{dm}=-rh_{2}\left[\frac{1}{E}+1\right]K\frac{\sin\alpha}{R_{f}} \tag{76}$$

$$\frac{dB_{1}}{dm}=2\left[\frac{ra_{3}}{A}+\frac{1}{B}+ra_{3}A+B-2\left(1+ra_{3}\right)\right]\frac{dB}{dm} \tag{77}$$

$$\frac{dB_{2}}{dm}=2\left[\frac{r}{C}+\frac{1}{D}+rC+D-2\left(1+r\right)\right]\frac{dC}{dm} \tag{78}$$

$$\frac{dB_{3}}{dm}=-2rh_{2}\left[\frac{1}{E}+E+2\right]K\frac{\sin\alpha}{R_{f}} \tag{79}$$

$$\frac{dA}{dm}=\frac{dB}{dm}=-Kh_{2}\frac{\sin\alpha}{R_{b}},\quad \frac{dC}{dm}=\frac{dD}{dm}=h_{2}\frac{\sin\alpha}{R_{d}} \tag{80}$$

2.4 Variation of crushing load

The variation of crushing load can now be found from the following relation:

$$P_{\theta}=\frac{d(W_{b\theta}+W_{c\theta})}{dz}=\frac{\frac{d}{d\theta_{1}}(W_{b\theta}+W_{c\theta})}{\frac{dz}{d\theta_{1}}} \tag{81}$$

where, $W_{b\theta}$ and $W_{c\theta}$ are the work done in bending and circumferential stretching in rotation of first and third limbs of fold upto θ_1 and second limb upto θ_2 given by Eqs. (12) and (40); and z is the crushing distance in the direction of the load which is given by:

$$z=h_{2}\left[\left\{1+K\left(1+a_{4}m\right)\right\}\cos\alpha-K\left(1+a_{4}m\right)\cos\left(\theta_{1}+\alpha\right)-\cos\left(\theta_{2}-\alpha\right)\right] \tag{82}$$

therefore,

$$\frac{dz}{d\theta_{1}}=h_{2}\left[K\left(1+a_{4}m\right)\sin\left(\theta_{1}+\alpha\right)+\sin\left(\theta_{2}-\alpha\right)\frac{d\theta_{2}}{d\theta_{1}}\right]=\dot{z}\ \text{(say)} \tag{83}$$

where,

$$\frac{d\theta_2}{d\theta_1} = \frac{K\cos(\theta_1+\alpha)}{\cos(\theta_2-\alpha)} \tag{84}$$

Using Eqs. (12), (40) and (83), Eq. (81) gives:

$$P_\theta = \frac{\pi f_y t_0^2}{\sqrt{3}\dot{z}}\left[\begin{array}{l}(a_1+2a_2+1)(R_1+mh_2\sin\alpha)+Kh_2(1-m-ma_2)\sin(\theta_1+\alpha)+2a_2h_2\sin\alpha\\ +\frac{d\theta_2}{d\theta_1}\left\{2R_1+h_2\left\{2(1-m+K)\sin\alpha+(1-2m)\sin(\theta_2-\alpha)\right\}\right\}+2a_2Kh_2\sin\alpha\end{array}\right]$$
$$-\frac{2\pi f_y t_0}{\dot{z}\sin^2\alpha}\left[\begin{array}{l}\left\{R_b^2A_1+R_f^2A_3\right\}\cos(\theta_1+\alpha)-\left\{R_b^2B_1+R_f^2B_3\right\}\frac{\sin 2(\theta_1+\alpha)}{2\sin\alpha}\\ -R_d^2\left\{-A_2\cos(\theta_2-\alpha)+B_2\frac{\sin(\theta_2-\alpha)}{2\sin\alpha}\right\}\frac{K\cos(\theta_1+\alpha)}{\cos(\theta_2-\alpha)}\end{array}\right] \tag{85}$$

3 Comparison with experimental observations

An Aluminium frustum, 1.85 *mm* thick, 130.3 *mm* long, and with end diameters of 43.9 and 57.5 *mm*, tested in axial compression [8] has been taken for experimental validation. The value of yield strength of the material of the frustum was found to be 92.0 *MPa*. The crushing load variation obtained experimentally for first fold has been plotted in Fig. 2. The values of size of fold was first determined numerically by minimizing the mean crushing load and this value was then used for finding out the variation of crushing load P_θ/P_0, where, $P_0 = \pi(R_1+R_2)\,tf_{yt}$, R_1 and R_2 are the end radii of frustum. The variation of crushing load for first fold taking $r =$ 1.0 has also been plotted in Fig. 2. The analytical load-deformation curve does not start from zero load level due to the neglect of the elastic deformation in the beginning. The post peak experimental curve is found to be close to the analytical curve.

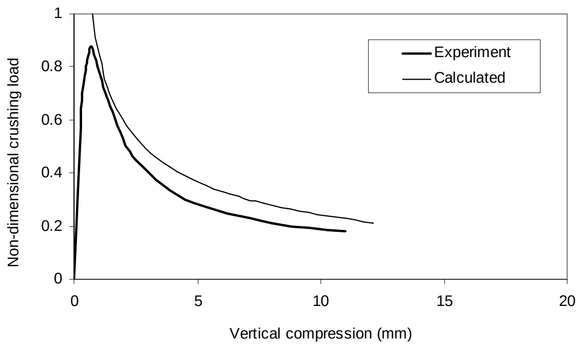

Figure 2: Load deformation curves for frustum

A steel cylindrical tube of 24.05 *mm* diameter and 1.01 *mm* thick tested in axial compression [12] has been used in the validation of the analysis presented in earlier sections. The value of yield strength of the material of the frustum was found to be 160.0 *MPa*. The values of size of fold and folding parameter were first determined numerically by minimizing the mean crushing load and these values were then used for finding out the variation of crushing load. The crushing load variation obtained experimentally and analytically for the first fold taking $r = 1.0$ have been plotted in Fig. 3. The post peak experimental curve is found to be close to the analytical curve.

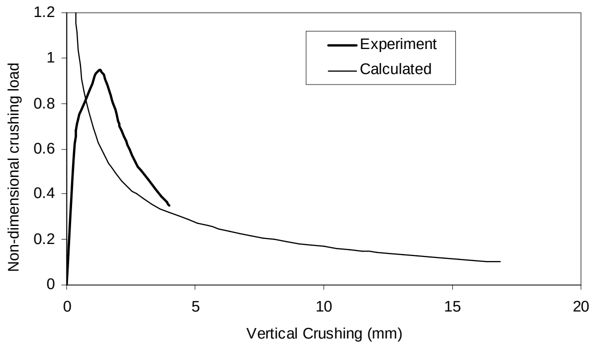

Figure 3: Load deformation curve of a steel tube

The influence of folding parameter on the non-dimensional mean crushing has been studied by plotting its variation in Fig. 4 for the first fold of the steel tube considered above. Each point on this curve corresponds to an optimal size of fold whose variation is also plotted in this figure. It is observed from this figure that the mean crushing load is maximum for total outside folding (i.e. $m = 0$) which reduces with increase in the value of m and after reaching an optimal value, it increases but the mean crushing load for the total outside folding (i.e. $m = 1$) is less than that of the total outside. The mean crushing load of the tube has two components, one due to bending and the other due to circumferential deformation. The variation of these two components has also been plotted in this figure. It is observed from their variation that for smaller values of folding parameter ($m < 0.5$), the energy absorption in bending is more than that in circumferential deformation but for larger values of folding parameter ($m > 0.5$), it is the vice versa. At the optimal point where folding parameter is slightly more than 0.5 ($m = 0.62$ for the tube considered here), the energy absorption in bending is slightly more than the circumferential deformation which for practical purposes may be taken to be almost equal.

A parametric study has also been carried out for studying the influence of the difference in the compressive and tensile strength of the material by taking the value of parameter r as 1.0, 1.5 and 2.0 for the steel tube considered above. The variation of mean crushing load with folding parameter for these values of r is plotted in Fig. 5. The value of the size of fold was first determined numerically by minimizing the mean crushing load, which was then used for finding out the mean crushing load. All the three curves in this figure start from the same mean crushing load at $m = 0$ because for this case of total outside folding, there is only extensional circumferential deformation and thus the value of r has no role to play. For the values of $m > 0$,

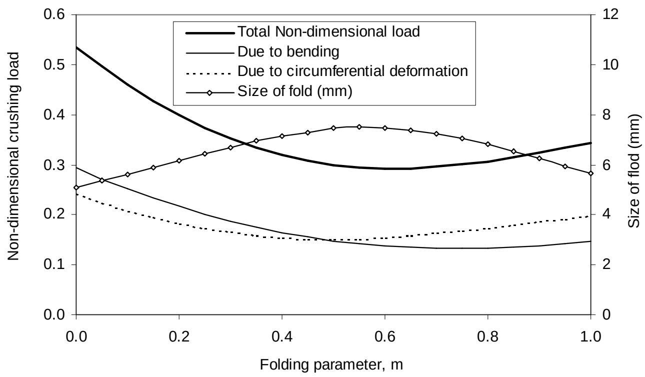

Figure 4: Variation of non-dimensional crushing load with folding parameter for steel tube with $r = 1$

the increase in the parameter r results in increase in the mean crushing load and decrease in the optimal value of folding parameter which is because of the material becoming stronger in compression thus the fold goes less inside the initial line.

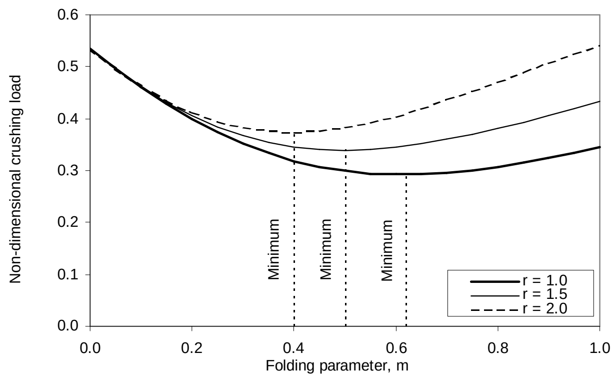

Figure 5: Variation of non-dimensional crushing load with folding parameter for steel tube with different values of r

4 Conclusions

An improved version of partly inside and partly outside straight fold model is developed for the axisymmetric axial crushing analysis of thin walled frusta. The existing total outside fold model of frusta and partly inside and partly outside fold model of tube can be derived from this model. The difference in the first and the subsequent folds has been highlighted and the same has been incorporated in the analysis. All the variables involved in the analysis have been computed mathematically. The variation in crushing load and the mean collapse load have been computed.

The results have been compared with experiments and reasonably good agreement has been observed. The results are of help in understanding the phenomenon of actual fold formation. For smaller values of folding parameter, the energy absorption in bending is more than that in circumferential deformation but for larger values of folding parameter, it is the vice versa. For optimal value of folding parameter, the energy absorption in bending is slightly more than the circumferential deformation, which for practical purposes may be taken to be almost equal. The consideration of material being stronger in compression as compared to tension results in increase in the mean crushing load and decrease in the optimal value of folding parameter.

References

[1] Mamalis AG and Johnson W. The quasi-static crumpling of thin walled circular cylinders and frusta under axial compression. *Int J Mech Sci*, 25:713–732, 1983.

[2] Abbas H, Paul DK, Godbole PN, and Nayak GC. Mathematical modeling of soft missile impact on protective walls. In *Proc. of the International Conference on Software Application in Engineering*, pages 577–580, India, 1989.

[3] Abbas H, Paul DK, Godbole PN, and Nayak GC. Soft missile impact on rigid targets. *Int. J. Impact Engng*, 16:727–737, 1995.

[4] Alexander JM. An approximate analysis of the collapse of thin cylindrical shells under axial loading. *Q.J. Mech. Appl. Math.*, 13(10-15), 1960.

[5] Jones N. Structural aspects of ship collisions. In Jones N, Wierzbicki T, et al., editors, *Structural crash-worthiness*, pages 308–337, London: Butterworth, 1983.

[6] Gupta NK. *Plasticity and impact mechanics.* New Age International (P) Limited Publishers, 1997.

[7] Gupta NK, Prasad GLE, and Gupta SK. Plastic collapse of metallic conical frusta of large semi-apical angles. *Int J Crash*, 2:349–366, 1997.

[8] Gupta NK and Abbas H. Axisymmetric axial crushing of thin frusta. *Thin-Walled Structures*, 36:169–179, 2000.

[9] Gupta NK and Abbas H. Mathematical modeling of axial crushing of cylindrical tubes. *Thin-Walled Structures*, 38:355–375, 2000.

[10] Gupta NK and Abbas H. Some considerations in axisymmetric folding of metallic round tubes. *Int. J. Impact Engng.*, 25:331–344, 2001.

[11] Gupta NK, Abbas H, and Hosseini M. Axi-symmetric crushing of thin frusta and tube. *Indian National Science Academy Journal.* India (In press).

[12] Gupta NK, Abbas H, and Venkatesh. Considerations in straight fold analysis of thin tube under axial compression. *Int. J. Impact Engng*, 31:1039–1053, 2005.

[13] Gupta NK and Velmurugan R. Consideration of internal folding and non-symmetric fold formation in axi-symmetric axial collapse of round tubes. *Int. J. Solids & Structures*, 34:2611–2630, 1997.

[14] Abramowicz W and Jones N. Dynamic axial crushing of circular tubes. *J. of Impact Engng*, 2:263–281, 1984.

[15] Johnson W and Mamalis AG. *Crashworthiness of vehicles.* Mechanical Engineering Publication Ltd., London, 1978.